**International Journal of Power Electronics and Drive System (IJPEDS)**
Vol. 17, No. 3, September 2026, pp. 1768~1779
ISSN: 2088-8694, DOI: 10.11591/ijpeds.v17.i3.pp1768-1779 

# Short-circuit analysis and protection coordination of a 33 kV phosphate plant distribution network

**Cheikhani Abdel Kader, Bamba El Heiba, Mohamed El Mamy Mohamed Mahmoud, Beibah Gleigume, Abdel Kader Mahmoud**
Applied Research Laboratory of Renewable Energy, Water and Environment (URA3E-EX CRAER), University of Nouakchott, Nouakchott, Mauritania

**Article Info**

***Article history:***

Received Jul 3, 2026
Revised Aug 11, 2026
Accepted Aug 19, 2026

***Keywords:***

Asymmetrical fault analysis
Fault current inversion
Industrial distribution networks
Protection coordination
Transient stability

**ABSTRACT**

This study presents a short-circuit and protection coordination analysis of a 33 kV/0.4 kV industrial distribution network supplying a phosphate processing plant in Mauritania. Using ETAP software, the system was modeled to evaluate fault behaviors based on IEC 60909 and IEC 60255-151 standards. The study assesses the existing protection architecture and proposes an optimized digital protection framework. Simulation results indicate that the initial symmetrical short-circuit current at the 0.4 kV busbar reaches 96.5 kA, exceeding the 25-36 kA breaking capacity of the legacy equipment by nearly 300%. The analysis also investigates single-line-to-ground faults, revealing a fault current inversion phenomenon driven by the solid grounding configuration. To address these vulnerabilities, the study proposes upgrading to 150 kA-rated high-breaking-capacity switchgear and implementing advanced negative-sequence protection (ANSI 46) and transformer differential protection (ANSI 87T). This work provides a practical diagnostic framework for mitigating asymmetrical faults and optimizing protection coordination in heavy-duty industrial clusters.

*This is an open access article under the CC BY-SA license.*

***Corresponding Author:***

Cheikhani Abdel Kader
Applied Research Laboratory of Renewable Energy, Water and Environment (URA3E-EX CRAER)
University of Nouakchott
Nouakchott, Mauritania
Email: cheikhaniabdelkader@mail.com

## 1. INTRODUCTION

The operational stability of modern industrial power systems is fundamentally predicated on the precision of fault analysis and the reliability of protection coordination schemes [1]. Efficient power distribution is critical for heavy industrial facilities, such as phosphate processing plants, which rely heavily on continuous operation to avoid severe economic and material losses [2]. As industrial facilities evolve, incorporating complex motor loads and intricate distribution architectures, reliance on conventional steady-state power flow and standard short-circuit methodologies has become increasingly inadequate [3], [4]. Network anomalies, such as phase-breakage and high-magnitude asymmetrical faults, pose severe risks of equipment failure, thermal degradation, and operational instability [5], [6].

The IEC 60909 standard continues to serve as the foundational international framework for calculating symmetrical and asymmetrical fault currents in three-phase AC systems [7]. Digital simulation platforms, notably ETAP, have consequently become indispensable tools for conducting fault-level calculations and optimizing relay settings in complex industrial environments [8], [9]. An important aspect in maintaining the integrity of the electrical system is the precise selection and provision of performance switches, protecting the network and staff from the potentially devastating effects of short-circuits [10]. Furthermore, robust disturbance management and fault diagnosis now demand a comprehensive understanding of asymmetrical network behavior and transient signatures [11]. In parallel, recent literature extensively investigates the critical role of neutral grounding configurations—specifically comparing solid versus resistive grounding methods—in shaping short-circuit dynamics. Research confirms that the low zero-sequence impedance paths inherent to solid grounding can drastically amplify single-line-to-ground fault magnitudes, occasionally causing them to exceed three-phase fault levels [12]. Because conventional electromechanical overcurrent relays are frequently inadequate for mitigating such severe asymmetrical anomalies, modern industrial standards increasingly advocate for the deployment of advanced digital intelligent electronic devices (IEDs) [13]. The integration of specialized protective functions, such as negative-sequence monitoring (ANSI 46) and transformer differential protection (ANSI 87T), has thus emerged as the state-of-the-art approach to ensuring selectivity and preventing thermal degradation under heavy dynamic load stresses [14].

While existing literature extensively covers standard overcurrent coordination [15], there is a growing need to analyze fault-limiting strategies and grid impacts using advanced network configurations [16]. Furthermore, optimizing the planning and operational reliability of industrial and isolated distribution grids requires robust empirical and simulation frameworks [17]. This study focuses on the practical diagnostic optimization of the BOFALE industrial network, moving beyond standard descriptive case studies. It provides a structured ETAP simulation framework covering multiple fault conditions. The primary contribution lies in diagnosing the non-compliant switchgear architecture and proposing an optimized digital protection scheme that improves system performance, reduces losses, and ensures compliance with industrial standards [18]. By identifying critical equipment vulnerabilities and deploying a multi-layer protection strategy, this research ensures system reliability and personnel safety. The findings offer a replicable blueprint for upgrading legacy industrial networks to meet modern safety compliance and operational resilience standards, contributing to the broader field of industrial power system protection [19], [20].

## 2. METHOD

To ensure clarity, methodological transparency, and exact reproducibility in accordance with international power engineering standards, this section details the step-by-step experimental and mathematical framework we applied to the modeled power system.

### 2.1. Research design/approach

In this study, we employ a deterministic, simulation-based case study design to evaluate short-circuit fault dynamics and optimize protection coordination in a heavy-duty industrial distribution network. We selected a digital simulation approach as it is highly appropriate and necessary to address our research problem; it enables us to precisely compute severe asymmetrical fault currents and iteratively test relay selectivity under extreme thermal and electrodynamic constraints without jeopardizing the physical infrastructure.

### 2.2. Materials/data sources

We conducted our study on the 33 kV/0.4 kV electrical distribution network supplying the BOFALE phosphate processing plant. We directly acquired the single-line diagram and network parameters from the facility’s operational data. The system materials and datasets we utilized comprise:

- Upstream grid: A main 33 kV supply source with a short-circuit capacity of 500 MVAsc and an X/R ratio of 10.
- Power transformers: Two primary step-down units (T2: 4000 kVA, Z = 6%; T4: 630 kVA). For both units, we utilize a Dyn11 vector group with the secondary neutral solidly grounded (Yn), establishing a low zero-sequence impedance return path.
- Induction motors: Downstream asynchronous process and drilling motors, which we modeled as a lumped capacity of 2.5 MVA (0.4 kV, cosΦ = 0.85, ILR/In = 6.5, subtransient reactance Xd'' = 16.7%).
- Cables: Copper conductors with XLPE insulation (3×240 mm², R1 = 0.0754 Ω/km, X1 = 0.0720 Ω/km).

By integrating this comprehensive baseline data, we ensured that our electrical transient analyzer program (ETAP) model accurately reflects real-world industrial conditions. The detailed technical parameters are summarized in Table 1.

### 2.3. Procedures/implementation steps

We systematically executed our experimental procedure through the following sequence:

- Data integration and network modeling: We constructed the BOFALE network topology within the ETAP simulation platform (Figure 1), incorporating legacy circuit breaker ratings and cable ampacity limits.
- Load flow analysis: We executed steady-state power flow algorithms to establish the pre-fault voltage profile and nominal current flows across all medium- and low-voltage busbars.
- Standard short-circuit simulation: We computed initial symmetrical, asymmetrical, and peak fault levels (three-phase and single-line-to-ground) following strict IEC 60909 guidelines.

- Asymmetrical fault analysis: We simulated an open-phase (Phase A) discontinuity to quantify transient voltage imbalances and the propagation of negative-sequence currents to downstream motor loads.
- Protection optimization: We configured digital intelligent electronic devices (IEDs) utilizing IEC standard inverse-time characteristics, followed by a rigorous coordination time interval (CTI) verification.

Table 1. Technical input parameters and network simulation data

| Network component | Parameter description | Design/operational value |
|---|---|---|
| Upstream grid | Nominal voltage ($V_{grid}$) | 33 kV |
| | Short-circuit power ($S_{sc}$) | 500 MVA |
| | X/R ratio | 10 |
| Main transformer (T2) | Nominal apparent power ($S_r$) | 4.0 MVA (upgraded) |
| | Voltage ratio ($V_{prim}/V_{sec}$) | 33 kV/0.4 kV |
| | Positive-sequence impedance ($Z_1$) | 6.0% (X/R = 7) |
| | Zero-sequence impedance ($Z_0$) | 5.1% (X/R = 7) |
| | Vector group/coupling | Dyn11 |
| | Primary grounding | Delta (ungrounded) |
| | Secondary grounding | Solidly grounded neutral ($Y_n$) |
| Medium voltage busbars | Nominal voltage | 33 kV |
| | Operational frequency | 50 Hz |
| Low voltage busbars (Bus 1 & Bus 2) | Nominal voltage | 0.4 kV (400 V) |
| | Continuous nominal current | 6300 A |
| Low voltage main cables | Conductor material/insulation | Copper/XLPE |
| | Cross-sectional area | 3 x 240 mm² |
| | Positive resistance ($R_1$) | 0.0754 Ω/km |
| | Positive reactance ($X_1$) | 0.0720 Ω/km |
| Downstream asynchronous Drilling motors | Total lumped load capacity | 2.5 MVA |
| | Nominal motor voltage | 0.4 kV |
| | Locked-rotor current ratio ($I_{LR}$ / $I_n$) | 6.5 |
| | Average power factor (cosΦ) | 0.85 (Lagging) |
| | Subtransient reactance ($X''_d$) | 16.70% |

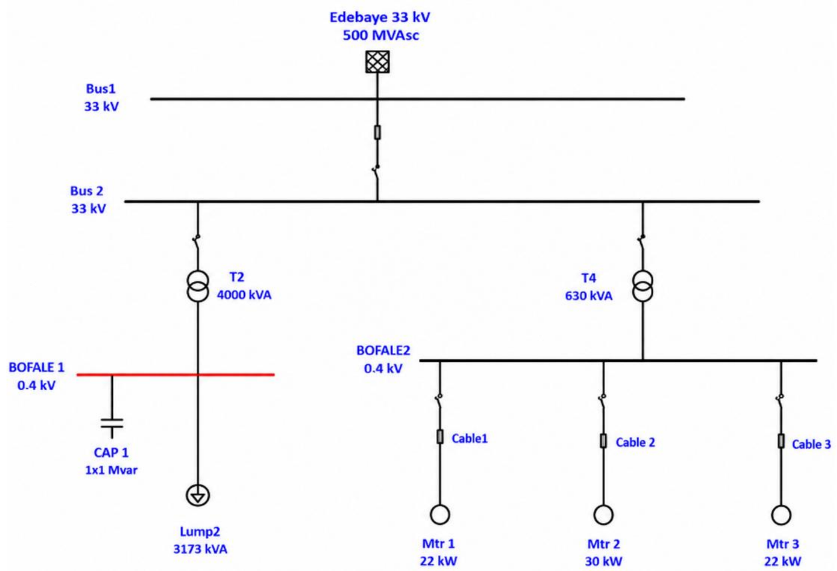


Figure 1. Baseline single-line diagram of the 33 kV/0.4 kV BOFALE distribution network modeled in ETAP

## 2.4. Models/algorithms/techniques

To guarantee the full reproducibility of our simulations, we based our mathematical and algorithmic core on standardized deterministic formulations:

### 2.4.1. Load flow program (Newton-Raphson method)

We determined the pre-fault network state variables (voltage magnitude $V_i$ and phase angle $\theta_i$) by solving non-linear power balance equations. For a network of N buses, the active ($P_i$) and reactive ($Q_i$) power injected at bus *i* are formulated as (1) and (2).

$$P_i = \sum_{j=1}^{N} V_i V_j \left(G_{ij} \cos\theta_{ij} + B_{ij} \sin\theta_{ij}\right) \quad (1)$$

$$Q_i = \sum_{j=1}^{N} V_i V_j \left(G_{ij} \sin\theta_{ij} - B_{ij} \cos\theta_{ij}\right) \quad (2)$$

We maintained convergence strictly below a tolerance threshold of 0.001 MW/Mvar.

### 2.4.2. Short-circuit calculation (IEC 60909)

We calculated the initial symmetrical short-circuit current ($I_k$") using an equivalent voltage source at the fault location, as in (3).

$$I_k'' = \frac{cU_n}{\sqrt{3}|Z_k|} \quad (3)$$

Where c is the voltage factor (we set this to 1.05 for maximum fault current stress and 0.95 for minimum thresholds), Un is the nominal system voltage, and Zk is the equivalent short-circuit impedance. To assess the electrodynamic withstand capability of the switchgear, we defined the peak short-circuit current ($i_p$) as (4).

$$i_p = \kappa\sqrt{2}I_k'' \quad (4)$$

Where kappa is the peak factor, which depends on the R/X ratio of the specific network branch.

### 2.4.3. Dynamic motor contribution

Following IEC 60909, we incorporated the dynamic subtransient contribution of large induction motors by replacing them at fault inception time (t = 0) with their subtransient internal impedance (ZM), as in (5).

$$Z_M = \frac{1}{I_{LR}/I_r} \times \frac{U_{rM}^2}{S_{rM}} \quad (5)$$

Where $I_{LR}$/Ir is the locked-rotor current ratio, UrM is the rated motor voltage, and SrM is the rated apparent power. Incorporating this subtransient reactance into the fault loop is essential, as neglecting dynamic contributions significantly underestimates the peak asymmetrical fault currents [21], [22].

### 2.4.4. Inverse-time relay operation (IEC 60255-151)

We mathematically defined the theoretical operating time (t) of our configured digital overcurrent and earth-fault relays as (6).

$$t = TMS \times \left(\frac{k}{(I/I_s)^{\alpha} - 1}\right) \quad (6)$$

Where time multiplier setting (TMS), I is the measured fault current, Is is the relay pick-up current setting, and the constants k and α define the specific curvature. To successfully override transformer magnetizing inrush currents and handle heavy motor starting transients, we applied IEC very inverse (k = 13.5, α = 1.0) and IEC extremely inverse (k = 80.0, α = 2.0) curves. Such custom inverse-time settings are widely recognized for maintaining tight coordination margins in industrial grids [13], [23]. We detail the comprehensive settings for our primary protection devices in Table 2.

Table 2. Comprehensive digital relay settings and protection architecture

| Relay ID | Protection function | CT ratio | Curve type (IEC) | Pickup (Is) | TMS/ time dial | Inst. threshold (I >>) | Additional settings |
|---|---|---|---|---|---|---|---|
| Relay 2 (T2 Incomer) | Phase (ANSI 51) | 8000/5 | Very inv. (VI) | 1.15×In | 0.25 | 10.0×In (0.05 s) | ANSI 87T enabled (slope: 25%) |
| | Earth fault (ANSI 51N) | 8000/5 | Extremely inv. (EI) | 0.20×In | 0.15 | 4.0×In (0.05 s) | - |
| Relay 4 (motor feeder) | Phase (ANSI 51) | 400/5 | Extremely inv. (EI) | 1.25×In | 0.10 | 8.0×In (0.02 s) | ANSI 46 (unbalance I_2 > 15%) |
| | Earth fault (ANSI 51N) | 400/5 | Extremely inv. (EI) | 0.10×In | 0.05 | 2.5×In (0.02 s) | - |
| Relay 7 (main 33kV) | Phase (ANSI 51) | 200/5 | Very inv. (VI) | 1.20×In | 0.45 | 12.0×In (0.10 s) | - |

## 2.5. Validation/evaluation strategy

We rigorously validated our proposed protection scheme using time-current characteristic (TCC) coordination plots generated via ETAP. For our evaluation criteria, we mandated a strict CTI of 0.35 s between downstream (primary) and upstream (backup) protection devices to ensure absolute selectivity and prevent cascading blackouts. Maintaining a CTI of 0.35 s aligns securely with established modern protection standards for industrial distribution systems [24]. Furthermore, we evaluated the ultimate short-circuit breaking capacity ($I_{cu}$) of our proposed high-performance switchgear against the computed initial symmetrical short-circuit current ($I''_k$) to guarantee strict safety compliance with the IEC 60947-2 standard.

### 2.6. Ethical considerations

Not applicable. Our research relies entirely on the deterministic software simulation of industrial electrical infrastructure and mathematical modeling. It does not involve human subjects, animal testing, or sensitive privacy data.

## 3. RESULTS AND DISCUSSION

To ensure clarity and address the specific dynamics of the BOFALE industrial network, this section is structured to present the simulation data objectively, followed by a detailed theoretical interpretation and a comparison with existing literature. The simulation results, conducted using ETAP software, are illustrated in Figures 2-7. Furthermore, the corresponding data are summarized in Tables 3-7.

### 3.1. Presentation of results

The simulation framework systematically evaluated the 33 kV/0.4 kV network across multiple contingency states to quantify severe voltage sags and current surges.

#### 3.1.1. Scenario A: Analysis of maximum fault current

Under a three-phase short circuit at the 0.4 kV BOFALE 1 busbar, as illustrated in Figure 2, the computed initial symmetrical RMS current ($I''_k$) reached 96.506 kA. The corresponding asymmetrical peak current ($i_p$) surged to 210.59 kA. This is heavily driven by the dynamic short-circuit contribution originating from the downstream induction motor cluster (Lump2), which is detailed in Tables 3(a) and 3(b).

#### 3.1.2. Scenario B: Analysis of sequence impedance and ground fault behavior

A single-line-to-ground (SLG) fault simulation, shown in Figure 3, yielded an initial symmetrical RMS current of 70.315 kA, which surprisingly exceeds the three-phase symmetrical fault current of 63.959 kA at the same location. This fault induced a severe voltage collapse, causing a 67.16% voltage sag on the 33 kV bus. The sequence impedances validating this condition are summarized in Tables 4(a) and 4(b).

#### 3.1.3. Scenario C: Impact of reactive power compensation

This scenario investigates the sensitivity of fault current levels to secondary system configurations, as modeled in Figure 4. Simulation results show a total magnitude fault current of 96.476 kA. Comparing this to the reference value (96.506 kA), the variation is negligible, confirming that the integration of capacitor banks has an imperceptible effect on the total short-circuit capacity, which is detailed in Tables 5(a) and 5(b).

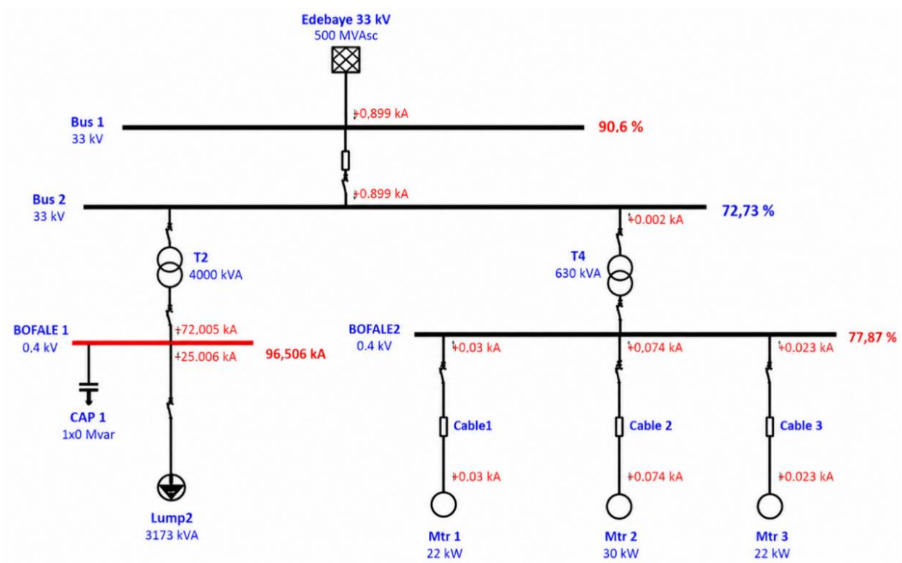


Figure 2. Short-circuit analysis of the 0.4 kV BOFALE 1 busbar: maximum contribution

Table 3. Maximum short-circuit current contribution for the 0.4 kV BOFALE 1 Busbar: (a) overall fault parameters and peak values using method C and (b) individual branch contributions and initial symmetrical RMS currents

(a)

| Parameter | Value | Unit | Observation |
|---|---|---|---|
| Fault type | 3-Phase fault | - | At bus BOFALE 1 |
| Nominal voltage | 0.4 | kV | |
| Voltage c factor | 1.05 | - | Maximum If |
| Peak value($i_p$) | 210.59 | kA | Method C |
| Steady state | 71.979 | kA RMS | |

(b)

| Contribution | | Voltage and initial symmetrical current (RMS) | | | | |
|---|---|---|---|---|---|---|
| From bus ID | To bus ID | %V From bus | Real (kA) | Imaginary (kA) | X/R ratio | Magnitude (kA) |
| BOFALE 1 | Total | 0 | 21.475 | -94.087 | 4.4 | 96.506 |
| Bus 2 | BOFALE 1 | 72.73 | 11.788 | -71.033 | 6 | 72.005 |
| Lump2 | BOFALE 1 | 105 | 9.686 | -23.054 | 2.4 | 25.006 |
| Bus1 | Bus 2 | 90.6 | 0.146 | -0.887 | 6.1 | 0.899 |
| BOFALE 2 | Bus 2 | 77087 | 0.001 | -0.001 | 0.7 | 0.002 |

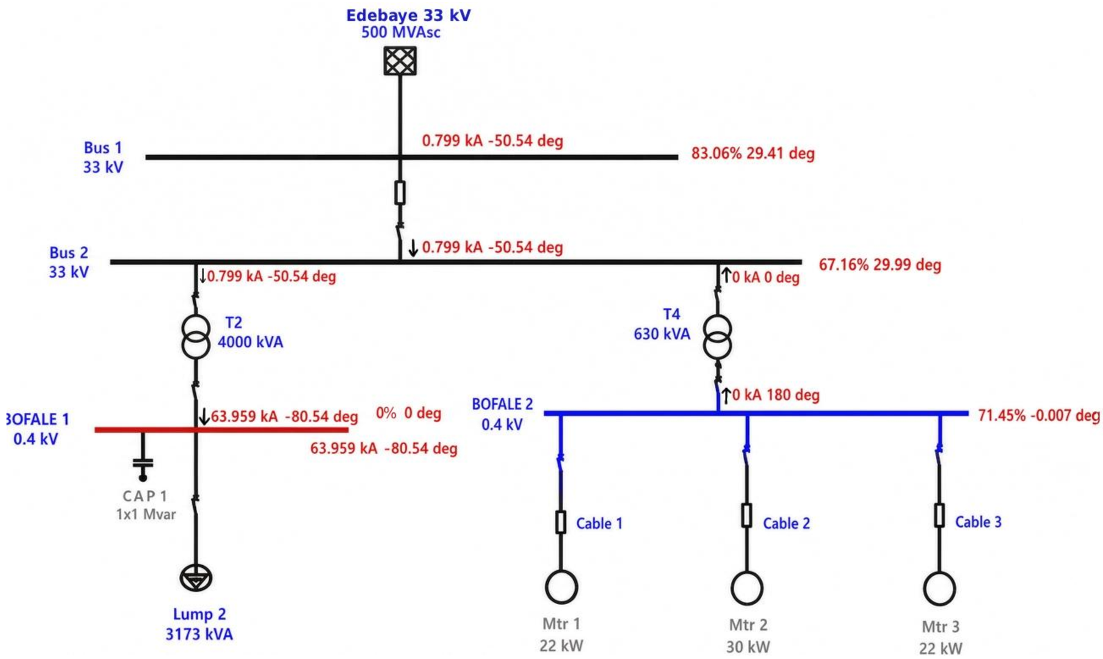


Figure 3. Minimum short-circuit fault analysis at the 0.4 kV Bofale 1 Busbar

Table 4. Minimum short-circuit analysis and sequence impedances (0.4 kV BOFALE 1 Busbar): (a) overall fault parameters and minimum c factor and (b) branch contributions for 3-phase and single line-to-ground faults alongside sequence impedance components

(a)

| Parameter | Value | Unit | Observation |
|---|---|---|---|
| Fault type | 3-Phase/SLG | - | At bus BOFALE 1 |
| Nominal voltage | 0.4 | kV | |
| Voltage c factor | 0.95 | - | Minimum $I_f$ |

(b)

| Contribution | | 3-phase fault | | SLG Fault (kA) | | | | | Positive & zero sequence impedances Looking into "From Bus" | | | |
|---|---|---|---|---|---|---|---|---|---|---|---|---|
| From Bus ID | To Bus ID | %V From Bus | 3-Phase Fault (kA) | % Voltage at From Bus Va | Vb | Vc | Ka Symm, RMS SLG Fault (kA) | 3I0 | % Impedance on 100 MVA BASE R1 | X1 | R0 | X0 |
| BOFALE 1 | Total | 0 | 63.959 | 0 | 90.7 | 90.65 | 70.3 | 70.315 | 3.31E+01 | 1.99E+02 | 2.42E+01 | 1.45E+02 |
| Bus 2 | BOFALE 1 | 67.16 | 63.959 | 78.8 | 92.2 | 78.82 | 70.3 | 70.315* | 3.31E+01 | 1.99E+02 | 2.42E+01 | 1.45E+02 |
| Bus1 | Bus 2 | 83.06 | 0.799 | 86.9 | 92.2 | 87.49 | 0.51 | 0 | 1.04E+02 | 1.07E+01 | | |
| BOFALE 2 | Bus 2 | 71.45 | 0 | 78.6 | 93.5 | 93.55 | 0 | 0 | | | | |

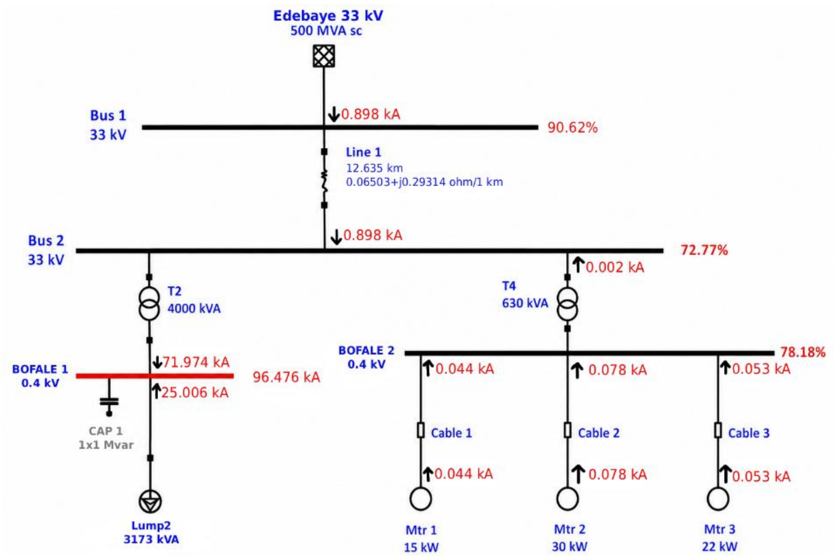


Figure 4. Short-circuit analysis of the 0.4 kV BOFALE 1 Busbar under asymmetrical fault conditions

Table 5. Asymmetrical short-circuit analysis for the 0.4 kV BOFALE 1 Busbar: (a) overall fault parameters and peak values and (b) individual branch contributions and initial symmetrical currents

(a)

| Parameter | Value | Unit | Observation |
|---|---|---|---|
| Fault type | 3-Phase fault | - | At bus BOFALE 1 |
| Nominal voltage | 0.4 | kV | |
| Voltage c factor | 1.05 | - | Maximum If |
| Peak value | 237.565 | kA | Method B |
| Steady state | 71.932 | kA RMS | |

(b)

| Contribution | | Voltage and initial symmetrical current (RMS) | | | | |
|---|---|---|---|---|---|---|
| From bus ID | To bus ID | %V From Bus | Real (kA) | Imaginary (kA) | X/R ratio | Magnitude (kA) |
| BOFALE 1 | Total | 0 | 21.471 | -94.057 | 4.4 | 96.476 |
| Bus 2 | BOFALE 1 | 72.77 | 11.785 | -71.003 | 6 | 71.974 |
| Lump2 | BOFALE 1 | 105 | 9.686 | -23.054 | 2.4 | 25.006 |
| Bus1 | Bus 2 | 90.62 | 0.146 | -0.886 | 6.1 | 0.899 |
| BOFALE 2 | Bus 2 | 78.18 | 0.001 | 0 | 0.3 | 0.001 |

### 3.1.4. Scenario D: Open-conductor fault analysis and voltage stability

A phase 'A' discontinuity on the 33 kV feeder, depicted in Figure 5, resulted in a 42.6% voltage collapse on the primary bus. This propagated downstream, resulting in a secondary distribution bus voltage of 0.243 kV (60.7% of the 0.4 kV nominal value), triggering significant negative-sequence currents across the asynchronous motors, with operational impacts detailed in Table 6.

## 3.2. Analysis and interpretation

The surge of the initial symmetrical RMS current to 96.506 kA (Scenario A) holds critical implications for facility safety. It exceeds the original 25–36 kA breaking capacity of the legacy switchgear by nearly 300%. This mathematically confirms that the current architecture is dangerously non-compliant with standard IEC 60909 fault tolerance thresholds [7].

Furthermore, to substantiate the fault current inversion observed in Scenario B ($I_{SLG} > I_{3\Phi}$), we must perform a sequence-network mathematical analysis. In symmetrical component theory, the three-phase short-circuit current depends exclusively on the positive-sequence impedance ($Z_1$):

$$I_{3\Phi} = \frac{c \cdot U_n}{\sqrt{3} \cdot Z_1} \tag{7}$$

Conversely, the single-line-to-ground fault current ($I_{SLG}$) is a function of the positive ($Z_1$), negative ($Z_2$), and zero-sequence ($Z_0$) impedances:

$$I_{SLG} = \frac{\sqrt{3} \cdot c \cdot U_n}{Z_1 + Z_2 + Z_0} \tag{8}$$

Assuming a bolted fault and $Z_1 \approx Z_2$ for static network components, the condition for $I_{SLG} > I_{3\Phi}$ dictates:

$$\frac{\sqrt{3}\cdot c\cdot U_n}{2Z_1+Z_0} > \frac{c\cdot U_n}{\sqrt{3}\cdot Z_1} \Rightarrow 3Z_1 > 2Z_1 + Z_0 \Rightarrow Z_1 > Z_0 \quad (9)$$

As empirically proven by the ETAP sequence impedance outputs in Table IV, the zero-sequence reactance ($X_0$ = 145.0%) is significantly lower than the positive-sequence reactance (X1 = 199.0%). This condition ($Z_1 > Z_0$) is physically fulfilled by the 4.0 MVA transformer (T2), which utilizes a Dyn11 vector group with a solidly grounded secondary neutral. This grounding topology provides a highly conductive zero-sequence return path, perfectly explaining the current inversion phenomenon.

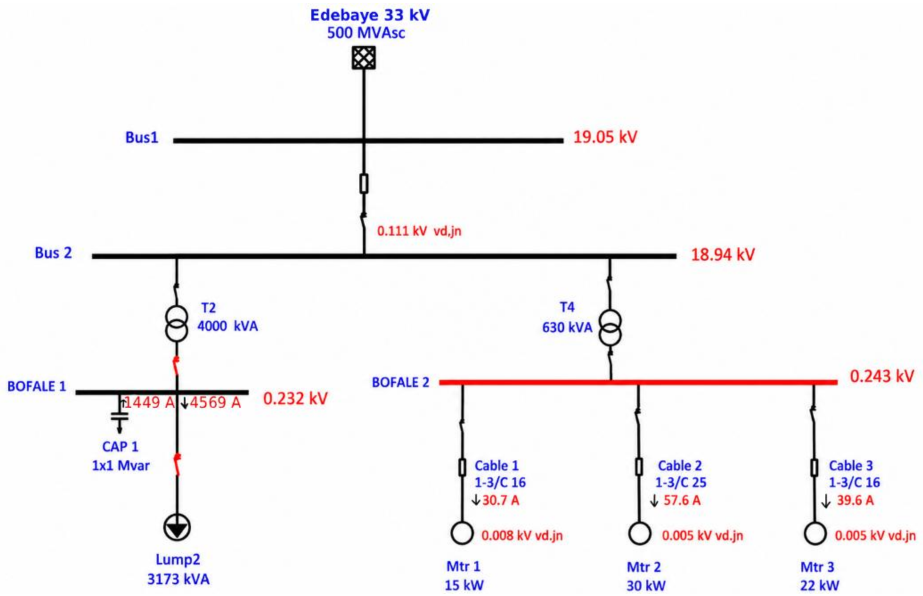


Figure 5. ETAP single-line diagram illustrating the phase 'A' discontinue ty and the resulting voltage imbalances

Table 6. Open-conductor asymmetry (phase A discontinuity)

| Parameter | Value | Unit | Observation/impact |
|---|---|---|---|
| Secondary distribution voltage | 0.243 | kV | Drops to 60.7% of nominal voltage |
| Negative-sequence voltage (V2) | >15 | % | High unbalance factor detected |
| Relay action required | ANSI 46 | - | Mandatory to isolate motor load |

### 3.3. Comparison with previous studies (state of the art)

The quantitative findings of this case study align tightly with recent advancements in power system protection [12]. The severe voltage sags and coordination challenges induced by dynamic motor contributions corroborate modern protection coordination schemes that highlight the inadequacy of conventional steady-state analyses in industrial microgrids [14], [25]. While existing literature extensively covers standard overcurrent coordination [15], this study provides empirical validation that solidly grounded industrial transformers can push asymmetrical faults beyond symmetrical thresholds, a phenomenon theoretically discussed but rarely quantified in legacy heavy-duty infrastructure optimization [19], [20].

### 3.4. Implications of findings and proposed

The theoretical and practical significance of these results mandates an immediate infrastructural upgrade at the BOFALE facility [18].

#### 3.4.1. Scenario E: Digital protection architecture

Relying on basic overcurrent elements is insufficient. The implementation of digital IEDs featuring negative-sequence monitoring (ANSI 46) and transformer differential protection (ANSI 87T) is required to guarantee selectivity and uninterrupted service continuity under extreme asymmetrical stresses [13], [14]. The proposed digital protection locations are illustrated in the single-line diagram of Figure 6.

#### 3.4.2. Scenario F: Protection coordination and infrastructure compliance

The operational effectiveness of the proposed scheme was validated through TCC analysis, as shown in Figure 7. We maintained a strict CTI of 0.35 s between the upstream and downstream relays. As detailed in Table 7, the network has been secured through the systematic replacement of non-compliant switchgear with high-performance air circuit breakers (ACB) rated at 150 kA ($I_{cu}$).

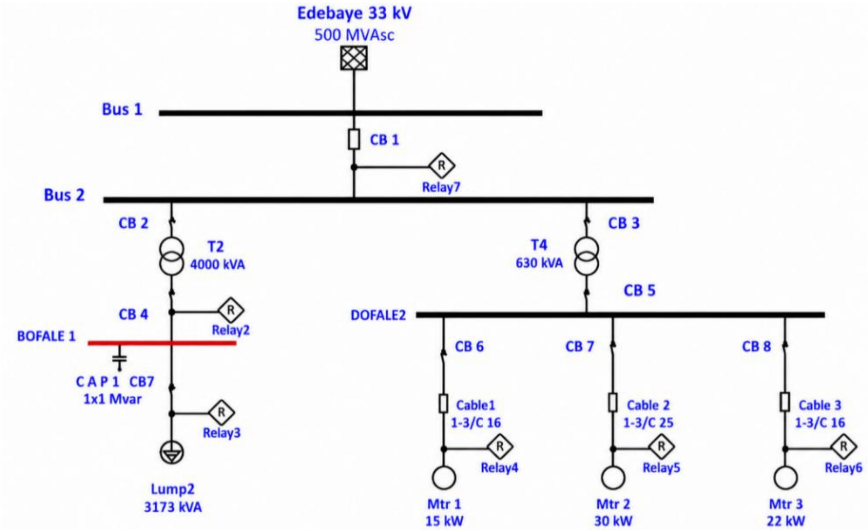


Figure 6. ETAP schematic modeling the occurrence of a phase 'A' open-circuit condition and the corresponding voltage asymmetry

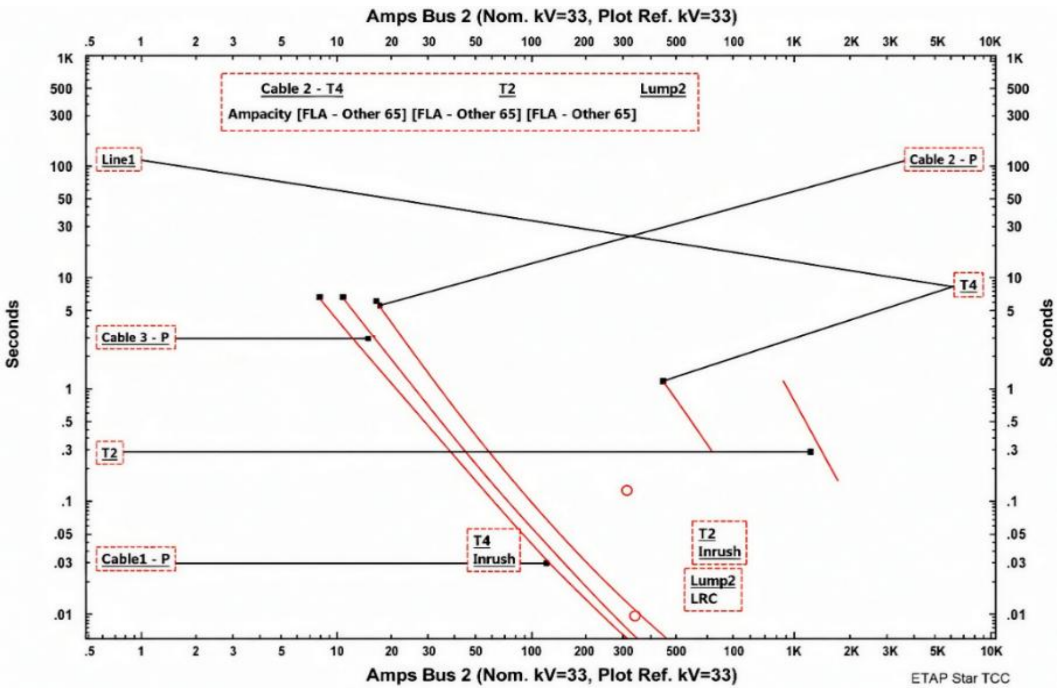


Figure 7. TCC curves

Table 7. Equipment compliance status before and after optimization

| Equipment | Placement | Ik″ (kA) | Initial state | Proposed Icu | Final state |
|---|---|---|---|---|---|
| CB1 | Main Incomer | 96.5 | Non-compliant | 150 kA | Compliant |
| CB2 | Feeder to T2 | 96.5 | Non-compliant | 150 kA | Compliant |
| CB3 | Feeder to T4 | 70.3 | Non-compliant | 100 kA | Compliant |
| CB4 | T2 Secondary | 96.5 | Non-compliant | 150 kA | Compliant |

## 4. CONCLUSION

In this work, a comprehensive, standard-compliant diagnostic framework was executed to evaluate the short-circuit behavior and protection coordination of the 33 kV / 0.4 kV BOFALE industrial distribution network. Shifting away from conventional steady-state assumptions, this study utilized ETAP software to systematically model the system's dynamic response to maximum symmetrical faults, asymmetrical ground faults, and open-conductor anomalies under IEC 60909 guidelines. Ultimately, a multi-layered digital protection architecture was designed to rectify severe legacy equipment non-compliances and ensure operational safety.

The investigation yielded critical empirical insights into legacy grid vulnerabilities. First, the initial symmetrical short-circuit current at the low-voltage busbar peaked at 96.5 kA, driven by a substantial 26% (25.0 kA) dynamic contribution from induction motors. This mathematically confirmed that the existing 25–36 kA switchgear was critically undersized and posed a severe safety hazard. Second, sequence-network analysis proved that the highly conductive zero-sequence path of the solidly grounded transformer induced a dangerous fault current inversion ($I_{SLG} > I_{3\Phi}$), pushing asymmetrical faults beyond symmetrical limits. To mitigate these extreme electrical and thermal stresses, the deployment of 150 kA-rated breakers alongside advanced digital relays (ANSI 46, ANSI 87T) was proposed, successfully restoring a robust coordination time interval (CTI) of 0.35 s.

While the study delivers a practical and replicable blueprint for upgrading heavy industrial networks, we acknowledge its inherent limitations. As a deterministic simulation based on a specific, single-site case study, the numerical thresholds derived are topologically dependent. Furthermore, the proposed architecture was evaluated solely within the ETAP simulation environment; it currently lacks a comparative sensitivity analysis across different grounding topologies and has not been validated through physical hardware-in-the-loop (HIL) experimental testing.

To build upon this foundational case study, future research will focus on a comparative sensitivity analysis evaluating solid grounding versus neutral grounding resistors (NGR) to optimize asymmetrical fault mitigation. Additionally, extending this analytical framework to incorporate adaptive protection strategies via IEC 61850 protocols and machine-learning-based fault diagnostics will be vital. Such advancements will facilitate the transition of legacy heavy-duty industrial clusters into resilient, smart microgrids capable of safely integrating distributed renewable energy resources.


## ACKNOWLEDGMENTS

The authors would like to express their gratitude to the Applied Research Laboratory of Renewable Energy, Water and Environment (URA3E-EX CRAER) at the University of Nouakchott for providing the scientific environment, technical resources, and favorable conditions necessary for the completion of this research.

## FUNDING INFORMATION

The authors hereby declare that no research grant, contract, financial support, or funding of any kind was received for the conduct of this research. The work was carried out independently without any external financial support.


## AUTHOR CONTRIBUTIONS STATEMENT

This journal uses the Contributor Roles Taxonomy (CRediT) to recognize individual author contributions, reduce authorship disputes, and facilitate collaboration.

| Name of Author | C | M | So | Va | Fo | I | R | D | O | E | Vi | Su | P | Fu |
|---|---|---|---|---|---|---|---|---|---|---|---|---|---|---|
| Cheikhani Abdel Kader | ✓ | ✓ | ✓ | ✓ | ✓ | ✓ | | ✓ | ✓ | ✓ | | | ✓ | |
| Bamba El Heiba | ✓ | | ✓ | ✓ | | | ✓ | | | ✓ | ✓ | | ✓ | ✓ |
| Mohamed El Mamy Mohamed Mahmoud | | ✓ | | | | ✓ | | ✓ | ✓ | ✓ | ✓ | ✓ | | |
| Beibah Gleigume | ✓ | | ✓ | ✓ | | | ✓ | | | ✓ | ✓ | | ✓ | ✓ |
| Abdel Kader Mahmoud | | | | | ✓ | | ✓ | | | ✓ | | ✓ | | ✓ |

C : **C**onceptualization
M : **M**ethodology
So : **So**ftware
Va : **Va**lidation
Fo : **Fo**rmal analysis
I : **I**nvestigation
R : **R**esources
D : **D**ata Curation
O : Writing - **O**riginal Draft
E : Writing - Review & **E**diting
Vi : **Vi**sualization
Su : **Su**pervision
P : **P**roject administration
Fu : **Fu**nding acquisition

## CONFLICT OF INTEREST STATEMENT

The authors declare no conflict of interest.

## DATA AVAILABILITY

The data presented in this article are fully illustrated by the provided tables, figures, and graphs. Supplementary data may be made available by the corresponding author upon reasonable request.

## REFERENCES


[1] A. M. Agwa and A. A. El-Fergany, "Protective relaying coordination in power systems comprising renewable sources: challenges and future insights," *Sustainability*, vol. 15, no. 9, p. 7279, Apr. 2023, doi: 10.3390/su15097279.

[2] K. V. Natkar and N. Kumar, "Short-circuit analysis of 220/132 kV substations by using ETAP," *International Journal of Advanced Technology in Engineering and Science*, vol. 4, no. 3, pp. 122–129, 2016.

[3] R. Tiwari, R. K. Singh, and N. K. Choudhary, "Coordination of dual setting overcurrent relays in microgrid with optimally determined relay characteristics for dual operating modes," *Protection and Control of Modern Power Systems*, vol. 7, no. 1, p. 6, Dec. 2022, doi: 10.1186/s41601-022-00226-1.

[4] Y.-Y. Hong, C.-W. Yu, Y.-D. Lee, J.-L. Jiang, and S.-S. Wang, "Coordination of protective relays in distribution systems considering uncertainty caused by renewables and demands based on orthogonal experiments," *Sustainable Energy, Grids and Networks*, vol. 36, p. 101206, Dec. 2023, doi: 10.1016/j.segan.2023.101206.

[5] A. Tariq, K. L. Khatri, M. I. U. Haque, M. A. Raza, S. Ahmed, and M. Muzammil, "Investigation of the effects of distributed generation on protection coordination in a power system," *Engineering, Technology & Applied Science Research*, vol. 11, no. 5, pp. 7628–7634, Oct. 2021, doi: 10.48084/etasr.4338.

[6] J. Schipper *et al.*, "Steady-state power system analysis revisited for hybrid AC–DC grids," *Renewable and Sustainable Energy Reviews*, vol. 215, p. 115564, Jun. 2025, doi: 10.1016/j.rser.2025.115564.

[7] International Electrotechnical Commission. IEC 60909-0, "Short-circuit currents in three-phase A.C. systems. Part 0, Calculation of currents," 2016.

[8] E. E. Omran *et al.*, "An adaptive protection scheme for an inverter-dominated grid considering Momentary Cessation," *Electric Power Systems Research*, vol. 244, p. 111594, Jul. 2025, doi: 10.1016/j.epsr.2025.111594.

[9] J. Oelhaf *et al.*, "A scoping review of machine learning applications in power system protection and disturbance management," *International Journal of Electrical Power & Energy Systems*, vol. 172, 2025, doi: 10.1016/j.ijepes.2025.111257.

[10] A. Kuriakose and S. Balamurugan, "Optimum overcurrent relay coordination in scaled-down IEEE 5-bus system for changing network configuration," *International Review of Electrical Engineering (IREE)*, vol. 19, no. 1, p. 31, Feb. 2024, doi: 10.15866/iree.v19i1.23915.

[11] B. Gleigume *et al.*, "Short-circuit analysis in a mini electrical grid using ETAP," *International Journal on Energy Conversion (IRECON)*, vol. 13, no. 3, p. 79, May 2025, doi: 10.15866/irecon.v13i3.25745.

[12] A. Chowdhury, K. Nayak, and A. K. Pradhan, "Positive sequence component based directional relaying for lines integrated with solar photovoltaic plant," *Electric Power Systems Research*, vol. 237, Art. no. 111022, 2024, doi: 10.1016/j.epsr.2024.111022.

[13] E. Sorrentino and J. V. Rodríguez, "Optimal coordination of directional overcurrent protections considering the occurrence probability of different configurations and the effect of grouping cases," *Electric Power Systems Research*, vol. 218, 2023, doi: 10.1016/j.epsr.2023.109163.

[14] H. J. Ashtiani, S. Naeiji, A. Shabani, and Z. J. Shen, "Supervised machine learning and current signal based universal fault protection strategy for distributed generation integrated into power systems," *2024 8th International Conference on Green Energy and Applications, ICGEA 2024*, pp. 43–47, 2024, doi: 10.1109/ICGEA60749.2024.10560987.

[15] S. Shaikh, S. Shaikh, A. M. Soomar, and S. H. H. Shah, "Coordination of protective relays in the substation," *International Journal of Power Electronics and Drive Systems (IJPEDS)*, vol. 14, no. 3, p. 1471, Sep. 2023, doi: 10.11591/ijpeds.v14.i3.pp1471-1478.

[16] A. Shah, "Impact of current limiting reactor on bulk power network – a case study," in *2023 IEEE Texas Power and Energy Conference (TPEC)*, IEEE, Feb. 2023, pp. 1–6. doi: 10.1109/TPEC56611.2023.10078670.

[17] K. Salihi, M. Q. Taha, A. Oubeidi, M. Ndongo, S. Ben Jabrallah, and B. El Heiba, "Planning optimization of a standalone photovoltaic/diesel/battery energy system for a gold mining location in Mauritania," *Engineering, Technology & Applied Science Research*, vol. 14, no. 4, pp. 15637–15644, Aug. 2024, doi: 10.48084/etasr.7776.

[18] M. Musaruddin *et al.*, "Optimizing network reconfiguration to reduce power loss and improve the voltage profile in the distribution system: A practical case study," *e-Prime - Advances in Electrical Engineering, Electronics and Energy*, vol. 8, p. 100599, Jun. 2024, doi: 10.1016/j.prime.2024.100599.

[19] A. S. Alhanaf, M. Farsadi, and H. H. Balik, "Fault detection and classification in ring power system with DG penetration using hybrid CNN-LSTM," *IEEE Access*, vol. 12, pp. 59953–59975, 2024, doi: 10.1109/ACCESS.2024.3394166.

[20] M. M. Zaben, M. Y. Worku, M. A. Hassan, and M. A. Abido, "Machine learning methods for fault diagnosis in AC microgrids: a systematic review," *IEEE Access*, vol. 12, pp. 20260–20298, 2024, doi: 10.1109/ACCESS.2024.3360330.

[21] F. Alasali *et al.*, "Highly sensitive protection scheme considering the PV operation control models," *Electric Power Systems Research*, vol. 237, 2024, doi: 10.1016/j.epsr.2024.111025.

[22] S. Dash, M. K. Jena, P. D. Achlerkar, and P. Shaw, "Exploring the interdependence between control and protection philosophies in inverter integrated power system: A case study on directional relaying schemes," *Electric Power Systems Research*, vol. 228, 2024, doi: 10.1016/j.epsr.2023.110074.

[23] F. Alasali *et al.*, "The recent development of protection coordination schemes based on inverse of AC microgrid: A review," *IET Generation, Transmission and Distribution*, vol. 18, no. 1, pp. 1–23, 2024, doi: 10.1049/gtd2.13074.

[24] S. Su *et al.*, "Adaptive current protection for three-phase short-circuit faults in active distribution networks," *IET Renewable Power Generation*, vol. 18, no. S1, pp. 4621–4637, 2024, doi: 10.1049/rpg2.13170.

[25] A. Chowdhury, S. Paladhi, and A. K. Pradhan, "Local positive sequence component based protection of series compensated parallel lines connecting solar photovoltaic plants," *Electric Power Systems Research*, vol. 225, 2023, doi: 10.1016/j.epsr.2023.109811.

## BIOGRAPHIES OF AUTHORS

**Cheikhani Abdel Kader** received his bachelor's degree in electromechanics and his master's degree in applied physics, specializing in renewable energy, in 2022. His research interests include the optimization of electrical networks. He can be contacted at email: cheikhaniabdelkader@gmail.com.

**Bamba El Heiba** has been a researcher and lecturer in the physics department at the University of Nouakchott, Mauritania, since 2019. Since 2018, he has been working at the Applied Research Unit for Renewable Energies 'URA3E', University of Nouakchott, Mauritania. He is interested in renewable energy resources and has published many papers regarding his research fields. He can be contacted at email: bmb.ahmed.heiba@gmail.com.

**Mohamed El Mami Mohamed Mahmoud** received his Ph.D. degree from Cheikh Anta Diop University (UCAD), Dakar, Senegal. Since 2020, he has been a lecturer in the Department of Physics at the University of Nouakchott, Mauritania. Since 2015, he has also been a researcher at the Applied Research Unit for Renewable Energies (URA3E) at the University of Nouakchott. His research interests primarily focus on renewable energy resources, their characterization, and their applications. He can be contacted at email: ouldabdelwehab@yahoo.fr.

**Beibah Gleigume** received his master's degree from the Higher Institute of Applied Sciences and Technology of Gabès, Tunisia, in 2022. His research interests include optimization of the electrical network. He can be contacted at email: beibah12a@gmail.com.

**Abdel Kader Mahmoud** received his Masters of Science in power stations in 1988 and his Ph.D. degree in electrical engineering from the Technical University of Tashkent in Uzbekistan in 1991. Then he received his second doctorate degree in renewable energy from the University of Cheikh Anta Diop (UCAD), Dakar, Senegal, in 2008. Currently, he is the manager of the Applied Research Laboratory of Renewable Energy (LRAER). He is the author and co-author of more than 30 scientific papers. He can be contacted at email: nakader@yahoo.fr.